# MRI Measures of Cortical Bone Water Concentration: Dependence on Age and Pore Volume Fraction

Alan C. Seifert[1], Cheng Li[1], Hamidreza Saligheh Rad[1], Chamith S. Rajapakse[1], Wenli Sun[1], Shing Chun Benny Lam[1], and Felix W. Wehrli[1]
[1]*Radiology, University of Pennsylvania, Philadelphia, PA, United States*

**Introduction:** Age-related increase in cortical bone porosity is a major cause of the impaired strength of osteoporotic cortical bone. The majority of these pores, however, are below the resolution limit achievable in vivo. Water $^1$H NMR signal in bone at 3T results from two compartments: long $T_2$ ($T_2 \geq 1$ ms), corresponding to free water in pores ('pore water'); and short $T_2$ ($T_2$ ~ 300-400 μs), corresponding to motionally restricted water bound to bone matrix collagen ('bound water') [1], as shown in Fig. 1. Ultrashort echo-time (UTE) MRI is able to detect the short-$T_2$ components in cortical bone [2] and enables measurement of bulk bone water content (BWC) [3], the sum of bound and pore water. BWC is expected to increase as pore volume expands, but because it is the sum of two components which change in opposite directions as bone tissue is lost, it is a less than optimal measure of bone health. The suppression ratio (SR), defined as the ratio of signal amplitudes without and with long-$T_2$ suppression (the red line in Fig. 1), may provide a better measurement of bone porosity. We quantify BWC in 72 human subjects and SR in 40 human subjects and 13 bone specimens, and compare these measurements to x-ray-based modalities.

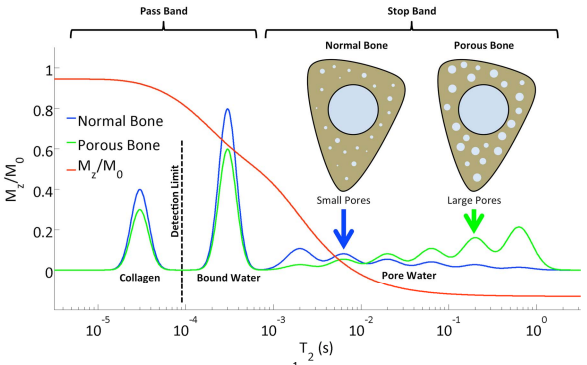


Fig. 1: General $T_2$ spectrum of bone $^1$H signal in normal and porous bone. Longitudinal magnetization ($M_z$) response to DB long-$T_2$ suppression pulse, which suppresses pore water while mostly sparing pore water, is shown in red.

**Methods:**

Human Subjects: BWC was quantified in 30 healthy men and 42 healthy women. SR was quantified in 40 females (34 from the BWC cohort). Scanning was performed at the left mid-diaphyseal tibia (38% of length proximal to lateral malleolus). Seven additional subjects (3 male, 4 female) underwent a series of 3 SR scans to quantify reproducibility.

Specimens: SR was quantified in 13 36-mm whole cross-section human tibial specimens, taken from the same 38%-length mid-diaphyseal location. Specimens were stored in phosphate-buffered saline in plastic tubes.

MRI: Human subjects were scanned on a 3T TIM Trio whole-body scanner (Siemens, Erlangen, Germany) using an 8-ch transmit/receive (T/R) knee coil, and specimens an elliptical birdcage T/R coil (both Invivo, Gainesville, FL). BWC was quantified relative to a known reference phantom using a 3D hybrid radial UTE method [4]. SR scans were acquired using a 2D slice-selective half-pulse UTE sequence with either no long-$T_2$ suppression, saturation using either a 15-ms 100°/110° water/fat dual-band saturation pulse (DB), or inversion recovery using a 1-kHz bandwidth 20-ms hyperbolic secant pulse with TI = 100 ms (IR) [5]. DB- and IR-SRs are given by the ratio of unsuppressed to long-$T_2$-suppressed images.

pQCT: A 2D image was acquired for each specimen and human subject with 0.4x0.4x2.3-mm$^3$ resolution using a Stratec XCT 2000 scanner (Orthometrix, White Plains, NY). BMD was quantified using the scanner software's in vivo tibial measurement protocol.

μCT: A 3D image of each specimen was acquired with 9-μm$^3$ isotropic resolution using a Bruker μCT scanner (Bruker, Kontich, Belgium), segmented, and binarized. Porosity was quantified as the ratio of pore volume to total volume, both excluding the endosteal cavity.

Analysis: Correlations were examined by least-squares regression.

| In Vivo | | | | | |
|---|---|---|---|---|---|
| | pQCT | BWC | IR SR | DB SR | |
| | $R^2$=0.31*** | $R^2$=0.22*** | $R^2$=0.44*** | $R^2$=0.45*** | Age |
| | | $R^2$=0.26*** | $R^2$=0.49*** | $R^2$=0.49*** | pQCT |
| IR SR | $R^2$=0.95*** | | $R^2$=0.23** | $R^2$=0.20* | BWC |
| Porosity | $R^2$=0.70*** | $R^2$=0.70*** | | $R^2$=0.96*** | IR SR |
| pQCT | $R^2$=0.28 | $R^2$=0.32* | $R^2$=0.56** | | |
| Age | $R^2$=0.82*** | $R^2$=0.76*** | $R^2$=0.57** | $R^2$=0.33* | |
| | DB SR | IR SR | Porosity | pQCT | |
| | | | Ex Vivo | | |

Table 1: Correlation matrix of in vivo and ex vivo measurements (*p<0.05, **p<0.005, ***p<0.0005).

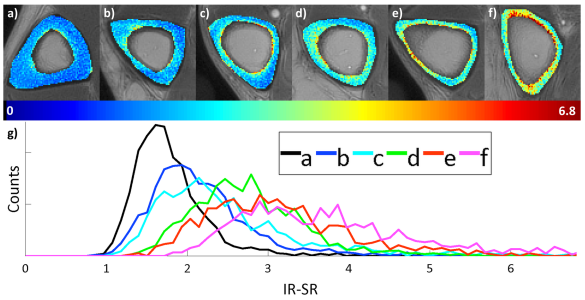


Fig. 2: Selected in vivo IR-SR colormaps overlaid on anatomical MR images (a-f), and IR-SR histograms, normalized by number of pixels (g).

**Results:** All examined correlations are given in Table 1. BWC increases 1.4%/decade ($R^2$=0.22, p<0.0005), though no correlation is observed in males alone (p>0.05). However, in vivo DB-SR and IR-SR are more strongly positively correlated with age ($R^2$=0.45, 0.44, respectively, p<0.0005) than is BWC. In specimens, porosity ($R^2$=0.57, p<0.005), DB-SR ($R^2$=0.82, p<0.0005), and IR-SR ($R^2$=0.76, p<0.0005) correlate strongly with age. Most importantly, SR is strongly correlated with porosity ($R^2$=0.70, p<0.0005). Elevated SR is more visible in the endosteal portion of the bone (Fig. 2), where structural degradation is commonly more severe. Both in vivo and ex vivo, the two SRs are very highly correlated ($R^2$=0.96, 0.95, respectively; both p<0.0005), and nearly interchangeable. Repeat studies of IR-SR yielded an average coefficient of variation of 2.2% and intraclass correlation coefficient of 0.99; DB-SR is similar.

**Discussion and Conclusions:** Smaller pores have a larger surface-to-volume ratio, resulting in shorter $T_2$ and possibly contributing to long-$T_2$-suppressed signal, as illustrated in Fig. 1. Larger pores, on the other hand, generate larger SRs, visible in the long upper tails in the histograms in Fig. 2g. Although this method does not yield an absolute measurement of pore volume fraction, the SR is more highly correlated with age and porosity than are either pQCT mineral density or BWC. The suppression ratio is a new, reproducible, and clinically practical biomarker for cortical bone porosity.

**References:** [1] Horch RA, et al. MRM 2010;64:680-7. [2] Robson MD, et al. J Comput Assist Tomogr 2003;27(6):825-46. [3] Techawiboonwong A, et al. NMR Biomed 2008;21:59-70. [4] Rad HS, et al. NMR Biomed 2011;24(7):855-64. [5] Li C, et al. MRM 2012;68(3):680-9.

**Acknowledgements:** NIH R01 AR50068, F31 AG042289, UL1TR000003, HHMI International Student Research Fellowship, and Institution's ITMAT.